



ASEISMIC ROOF ISOLATION SYSTEM BUILT WITH STEEL OVAL DAMPERS

Roberto VILLAVERDE¹, Manuel AGUIRRE², and Charles HAMILTON¹

SUMMARY

Presented here are the details of and results from experimental and analytical studies conducted to assess the feasibility and effectiveness of a proposed roof isolation system whose purpose is to reduce the seismic response of buildings. The proposed roof isolation system entails the detachment of a building's roof through the insertion of a low-friction mechanism and the attachment of oval-shaped steel dampers placed between the detached roof and the structure below. The objective is to form a simple resonant oscillator with the building's roof and these oval dampers, where the roof provides the oscillator's mass and the oval dampers its spring and damping elements. An additional objective is to induce a large number of inelastic deformation cycles into the oval dampers and make them, as a result, dissipate a large portion of the energy transmitted to a building during an earthquake. Through their stable hysteretic behavior, steel oval dampers have been found to work effectively as energy dissipating devices. In the experimental study, a small five-story steel frame is tested on an earthquake simulator alternatively with and without the proposed roof isolation system. Then, a comparison is made between the peak floor accelerations and story drifts induced in the frame in each case. In the analytical study, a typical thirteen-story building is similarly tested through numerical simulations. In both studies, the tests are conducted under the effect of different earthquake ground motions. In both studies, too, it is found that the proposed roof isolation system is effective in reducing the seismic response of the tested structures. It is concluded that the investigated system has the potential to become an inexpensive and effective way to protect some buildings against earthquake effects and reduce, as a result, the amount of structural and nonstructural damage they may experience during a strong earthquake.

INTRODUCTION

As demonstrated by the recent catastrophic events in Turkey, Taiwan, and India, earthquakes continue to be one of the most devastating forces in nature. Much progress has been made by the engineering community to mitigate the effect of these forces on the built environment, but many older buildings in the world's seismic regions do not meet modern design and construction standards and are thus highly vulnerable to earthquake damage. Although in principle it is possible to upgrade these older buildings to

¹ Civil Eng. Dept., University of California, Irvine, Calif., 92697, U.S.A. Email: rvl@eng.uci.edu; cham-ilty@uci.edu

² Instituto de Ingeniería, Univ. Nac. Aut. Mex., 04510 México, D.F., Mexico. Email: mag@pumas.iingen.unam.mx

the “belt-type” device has been already used in practical applications such as in the Restello Viaduct and two other bridges in the Autostrada system in Italy (Parducci and Medeot [11]; Medeot [12]).

This paper reports the details and results of experimental and analytical studies which are conducted to shed some light onto the behavior of a roof isolation system implemented with steel oval dampers and to investigate the effectiveness of such a system in reducing the earthquake response of buildings. Also reported here is the procedure used to determine the dimensions and properties of the oval dampers considered in the experimental and analytical studies.

EXPERIMENTAL STUDY

In the experimental study, a small steel frame is tested on a shake table alternatively with and without the proposed roof isolation system. Then, a comparison is made between the peak floor accelerations and story drifts induced in the frame in each case. In addition, complementary numerical simulations and experimental tests are carried out to (a) determine the maximum deformation and number of cycles the oval dampers would be subjected to during the shaking table tests; and (b) define the dimensions and characteristics of the oval dampers that would work effectively for the experimental model.

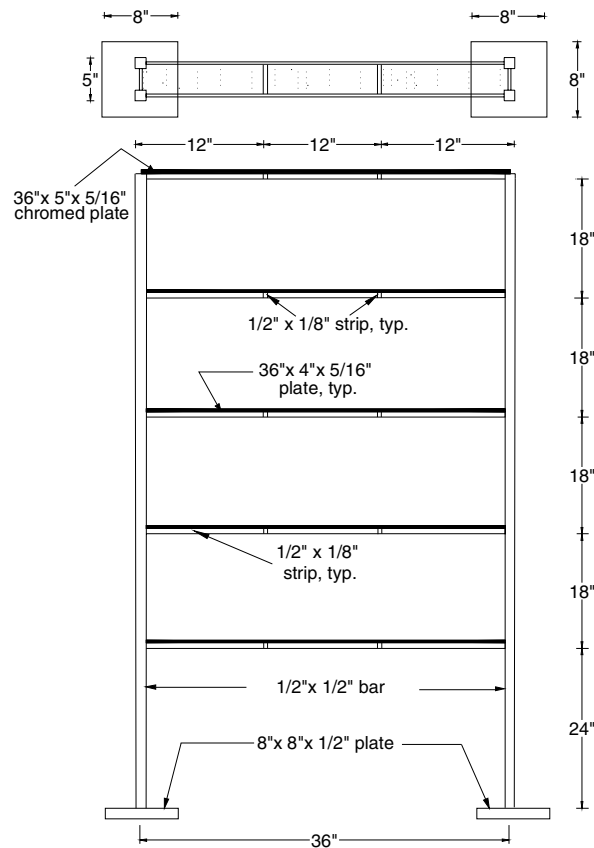


Figure 2. Configuration and dimensions of steel building model used in shake table tests

Experimental Model

The specimen used in the shaking table tests is the moment-resisting steel frame depicted in Figure 2. It has five stories, a height of 2.44 m (8 feet), and a width of 0.91 m (36 in). It is built by welding its square columns to base plates, welding its longitudinal and transverse rectangular beams to the columns, and welding its rectangular secondary beams to the longitudinal beams. Its floor plates are supported freely by all the beams, but are restrained against lateral motion by a small weld that joins them to one of the trans-

verse beams. Cold-rolled structural steel with a yield stress of 517.5 MN/m^2 (75 ksi) is used for the columns and the transverse beams. The longitudinal beams are built with hot-rolled structural steel with a yield stress of 248 MN/m^2 (36 ksi). The columns have a moment of inertia and a yield moment of 2169 mm^4 (0.00521 in^4) and 84.9 N-m (750.2 lb-in), respectively. The corresponding values for the longitudinal beams are 541 mm^4 (0.00130 in^4) and 21.8 N-m (192.4 lb-in). Small weights are added to the plates of the first, second, third, and fourth floors to adjust the fundamental natural frequency of the frame to a value of about 2.0 Hz; that is, a natural period equal to the number of floors divided by ten. The total weight of the frame without its base plates is 521.1 N (117.0 lb). Its top plate alone weighs 82.8 N (18.6 lb). In its conventional configuration, the frame exhibits a fundamental natural frequency of 2.0 Hz and a damping ratio of 2.8 percent. Without its top plate, the frame's fundamental natural frequency is 2.315 Hz and its damping ratio is 2.4 percent.

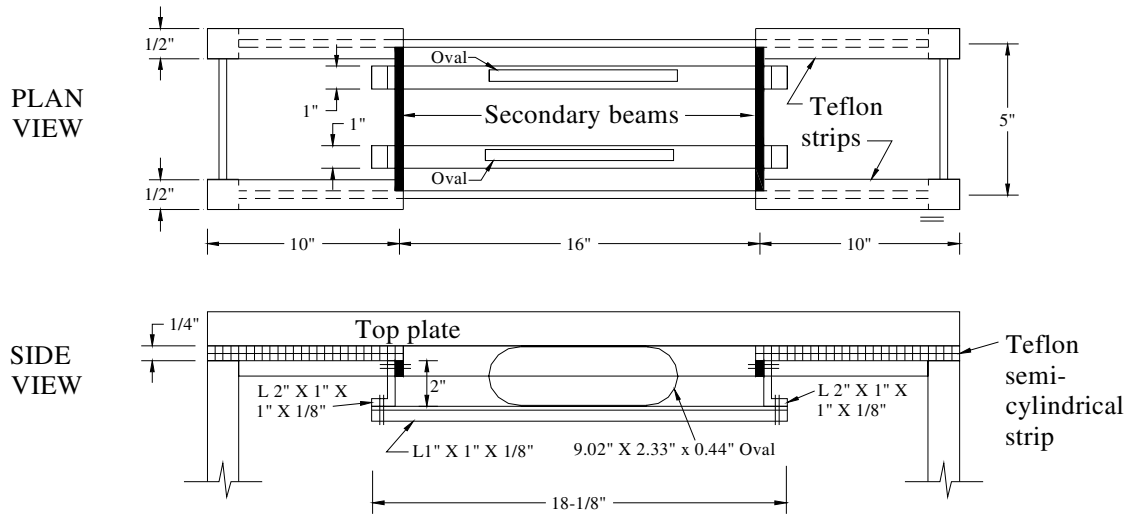


Figure 3. Roof isolation and oval connection details

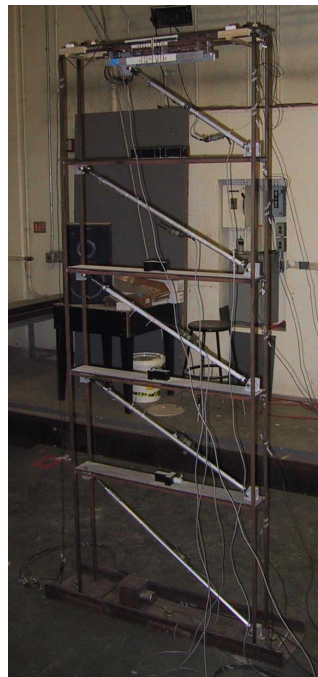


Figure 4. Steel frame mounted on shake table

For the implementation of the proposed roof isolation system, the top plate is released and mounted on four semi-cylindrical Teflon strips. In addition, it is connected to two steel oval dampers. The Teflon strips are supported by wooden guides, which in turn are supported by the fifth-floor longitudinal beams. The oval dampers are connected to and supported by two angles, themselves supported by two other angles that are connected to the secondary beams of the fifth-floor. To minimize the friction between the top plate and the Teflon strips, the top plate is chromed. Figure 3 presents the details of the mounting and isolation techniques used. Figure 4 shows a photograph of the roof-isolated frame and the way the frame is mounted on the shake table.

Selection of Steel Oval Dampers

The primary consideration in the selection of the properties and dimensions of the steel oval dampers needed to isolate the roof of the experimental model is the requirement of forming with the model's roof and the oval dampers an oscillator in resonance with the rest of the model. The ovals' properties and dimensions are thus selected in a way that makes them have an initial stiffness equal to the stiffness that is needed to make the natural frequency of such an oscillator equal to the fundamental natural frequency of the experimental model without its roof; that is, an initial stiffness equal to $[2\pi(2.315)]^2(18.6/386.4) = 10.18 \text{ lb/in}$ (1.785 kN/m). Another important consideration is to insure that the selected oval dampers are capable of resisting a large number of large-deformation cycles. To achieve this objective, the criterion suggested by Aguirre and Sánchez [6] is followed, supplemented with numerical simulations and experimental tests. Specifically, the properties and dimensions of the oval dampers are determined as follows:

(1) Based on the results of preliminary simulations with a numerical model of the roof-isolated frame, an estimate is made of the force the ovals would be subjected to during the shake table tests.

(2) A computer simulation is performed with a numerical model of the roof-isolated frame in which the ovals are modeled with a bilinear force-deformation behavior conceived on the basis of the required initial stiffness and the force estimated in Step 1. This simulation shows, among other results, the maximum oval deformation to be expected.

(3) Based on the force obtained in Step 1 and the true stress σ estimated from simple-tension tests of the steel grade chosen to build the ovals for an assumed strain of 1%, the ovals' width, thickness, and bend radius are selected to satisfy the following relationship derived by Aguirre and Sánchez [6]:

$$P = \frac{\sigma b e^2}{2R} \quad (1)$$

where P is the maximum force a single oval is capable of developing (when four plastic hinges are fully formed in the oval); and b , e , and R respectively denote the aforementioned width, thickness, and bend radius.

(4) An oval specimen is built with the selected dimensions and steel grade, and long enough to accommodate the deformation obtained in Step 2.

(5) The specimen is tested to determine its force-deformation characteristics, with its stiffness being among these characteristics.

(6) The width b is adjusted to obtain the required initial stiffness.

(7) Based on the test data of Step 5 and the adjusted width, a bilinear model is formulated to characterize the force-deformation behavior of the selected ovals.

(8) A computer simulation is carried out with the numerical model of the roof-isolated frame and the bilinear force-deformation model formulated in Step 7 to estimate the maximum deformation the ovals would be subjected to during the shake table tests.

(9) The ovals' length is established by considering that the straight portion of an oval should be approximately equal to 1.35 times the maximum deformation obtained in Step 8 plus a short addition (20 mm in this case) to accommodate the oval fasteners (practical rule proven effective to prevent undesirable oval distortion).

(10) To determine the selected ovals' fatigue life, specimens are constructed according to the dimensions established in Steps 3, 6 and 9 and tested under deformation cycles with amplitude equal to the

maximum deformation obtained in Step 8. If the fatigue life is deemed satisfactory, the selected oval dimensions are accepted as final.

Following the procedure described above, it is found that two ovals made with SAE 1010 ($\sigma_y = 26$ ksi) 24-gage sheet metal and the dimensions shown in Figure 5 provide the stiffness needed to effectively isolate the roof of the experimental model and resist, at the same time, the imposed deformation cycles without distortions or a premature fatigue failure. Each oval exhibits a force-deformation behavior that may be approximated by the bilinear model shown in Figure 6, where the coordinates of points K and M are (12.3 mm, 10.98 N) [(0.484 in, 2.467 lb)] and (103 mm, 12.6 N) [(4.06 in, 2.829 lb)], respectively. The experimentally obtained fatigue life of each oval (under a ductility demand of $115/12.3=9.3$, and a strain $\epsilon = 0.0104$) is 1900 cycles at a deformation amplitude of ± 115 mm (4.53 in), which corresponds to the peak oval deformation that is obtained from a computer simulation with a numerical model of the roof-isolated frame under 2.5 times the modified SCT record described in the following section. The force-deformation behavior shown in Figure 6 is used to model the ovals in this simulation. Note that ductility demand is defined here as the ratio of peak deformation to peak elastic deformation, and the strain is given by $\epsilon = e/2R$ (Aguirre and Sánchez [6]). Note also that ductility demand and strain are the two parameters that most significantly affect an oval's fatigue life; and that a combination of a high ductility demand (about 10) and a high strain (roughly 0.15) drastically shortens this fatigue life.

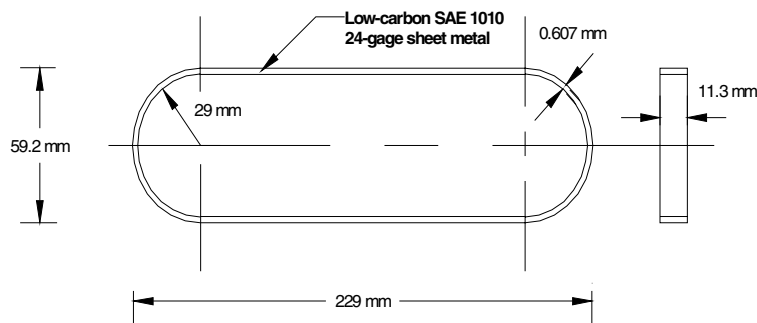


Figure 5. Dimensions of ovals used in roof isolation of experimental model

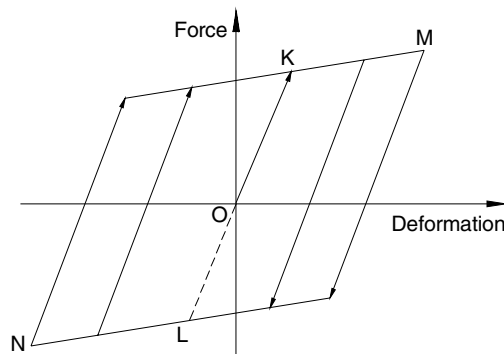


Figure 6. Approximate force-deformation behavior of oval dampers in experimental model

Shake Table Tests

The steel frame shown in Figure 4 is tested on the UCI shaking table with and without the proposed roof isolation system, recording the floor accelerations and story drifts in each case. Two tests are conducted. In the first test, the base of the specimen is subjected to a modified version of the SCT ground acceleration record from the 1985 Mexico (Michoacán) earthquake. This modified version is obtained by truncating the first 20 seconds of the record and by considering only the following 104 seconds. In addition, the time

axis is scaled by a factor of 0.216 to tune the accelerogram's dominant frequency to 2.315 Hz, the experimentally determined fundamental natural frequency of the frame without its top plate. The accelerations are also scaled up to obtain a peak acceleration of 0.257 g. The record is tuned to the fundamental natural frequency of the model without its roof because, as pointed out by Villaverde and Koyama [13], the effectiveness of a vibration absorber incorporated into a structure is more evident when the structure is subjected to a resonant (i.e., damaging) ground motion than when it is subjected to a ground motion that only induces a low-level response. The second test is performed using the N250° Anderson Dam acceleration record from the 1984 Morgan Hill earthquake, scaled down to a peak acceleration of 0.257 g. In this case, the record is not tuned to the natural frequency of the frame without its top plate because one of its dominant frequencies is already close to that frequency.

Some of the results from the shaking table tests are shown in Figures 7 through 11 and Table 1. Figures 7 and 8 show the story drifts experienced by the fifth story of the frame when tested with and without the proposed roof isolation system. Figure 7 shows the story drifts recorded when the test is conducted with the modified SCT record from the 1985 Mexico earthquake, while Figure 8 shows those recorded when the test is carried out with the scaled-down Anderson Dam record from the 1984 Morgan Hill earthquake. The accelerations at the level of the frame's fifth-floor beams are shown in Figures 9 and 10 for the cases when the frame is tested with and without the roof isolation system. Figure 9 depicts the accelerations obtained during the test performed with the accelerogram from the 1985 Mexico earthquake, while Figure 10 shows those attained when the test is conducted with the accelerogram from the 1984 Morgan Hill earthquake. The drifts experienced by the isolated roof during each of the two tests are shown in Figure 11. Table 1 summarizes the performance of the roof isolation system. This table lists the peak story drifts observed at each story during such two tests. It also gives the percentages by which these peak values are reduced when the frame is implemented with the roof isolation system.

Table 1. Peak story drifts in experimental frame with and without roof isolation system

| Story | 1985 Mexico earthquake | | | 1984 Morgan Hill earthquake | | |
|-------|------------------------|---------------------|---------------|-----------------------------|---------------------|---------------|
| | Without isolation (in) | With isolation (in) | Reduction (%) | Without isolation (in) | With isolation (in) | Reduction (%) |
| 5 | 0.314 | 0.148 | 53 | 0.230 | 0.152 | 34 |
| 4 | 0.455 | 0.206 | 55 | 0.343 | 0.215 | 37 |
| 3 | 0.570 | 0.261 | 54 | 0.430 | 0.278 | 35 |
| 2 | 0.575 | 0.260 | 55 | 0.433 | 0.284 | 34 |
| 1 | 0.426 | 0.194 | 55 | 0.332 | 0.214 | 36 |

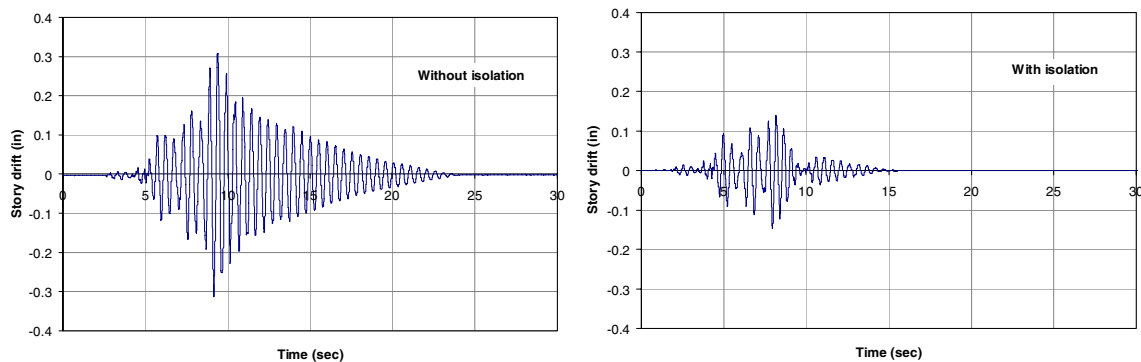


Figure 7. Fifth-story drifts in experimental frame without and with roof isolation system during shake table test with modified version of accelerogram from 1985 Mexico earthquake

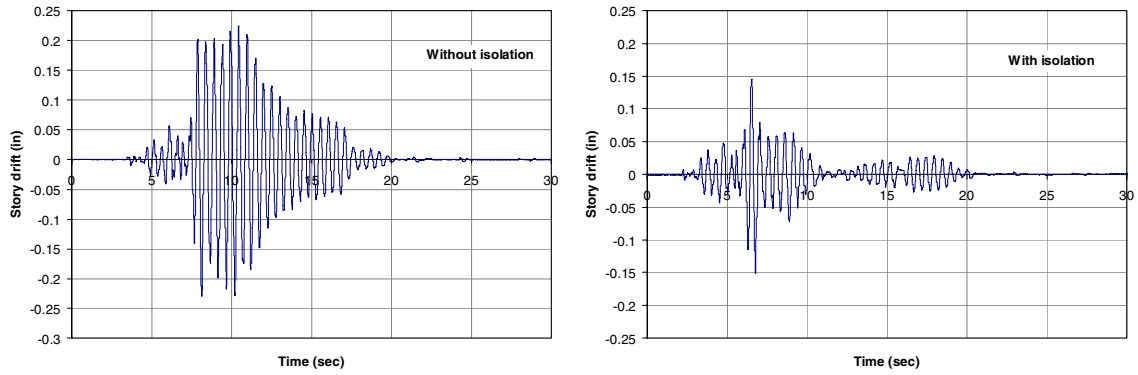


Figure 8. Fifth-story drifts in experimental frame without and with roof isolation system during shake table test with modified version of accelerogram from 1984 Morgan Hill earthquake

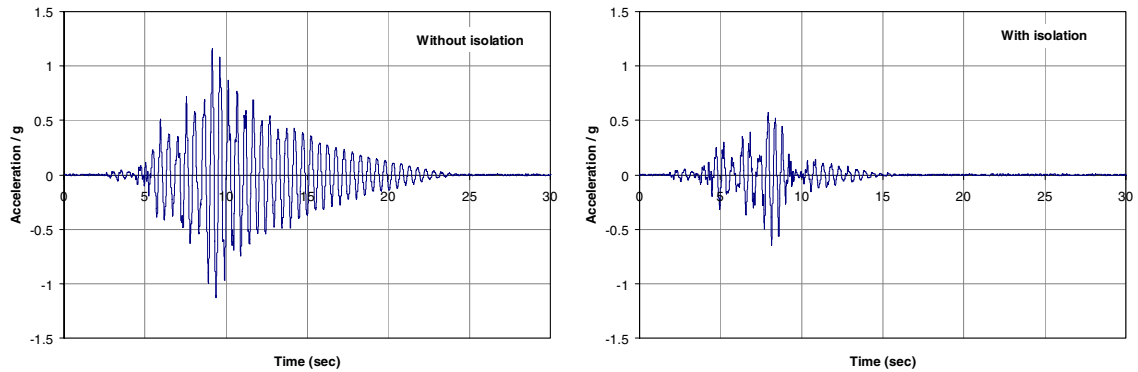


Figure 9. Fifth-floor accelerations in experimental frame without and with roof isolation system in shake table test with modified version of accelerogram from 1985 Mexico earthquake

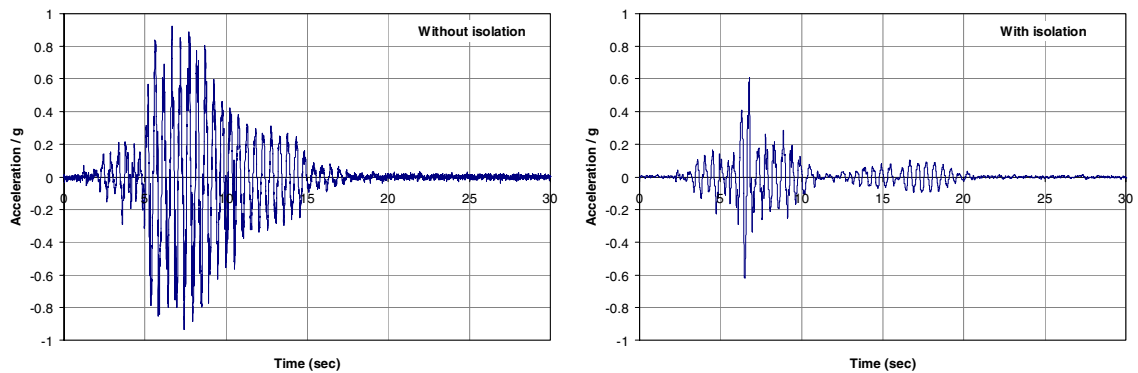


Figure 10. Fifth-floor accelerations in experimental frame without and with roof isolation system in shake table test with modified version of accelerogram from 1984 Morgan Hill earthquake

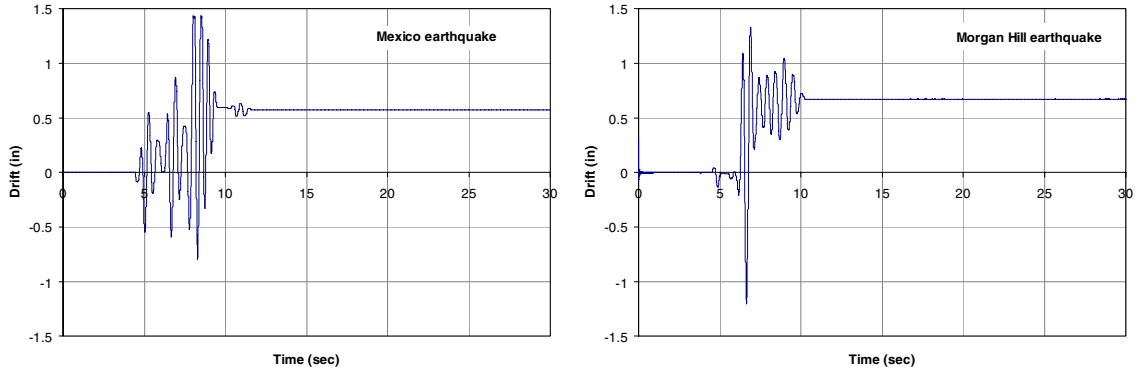


Figure 11. Drift of isolated roof in experimental frame with roof isolation system during tests with modified versions of accelerograms from 1985 Mexico and 1984 Morgan Hill earthquakes

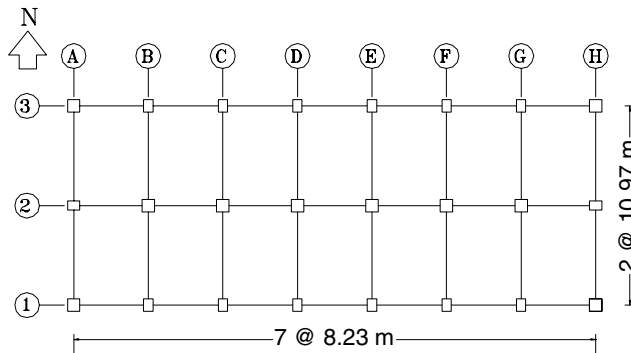


Figure 12. Plan view of studied building structure

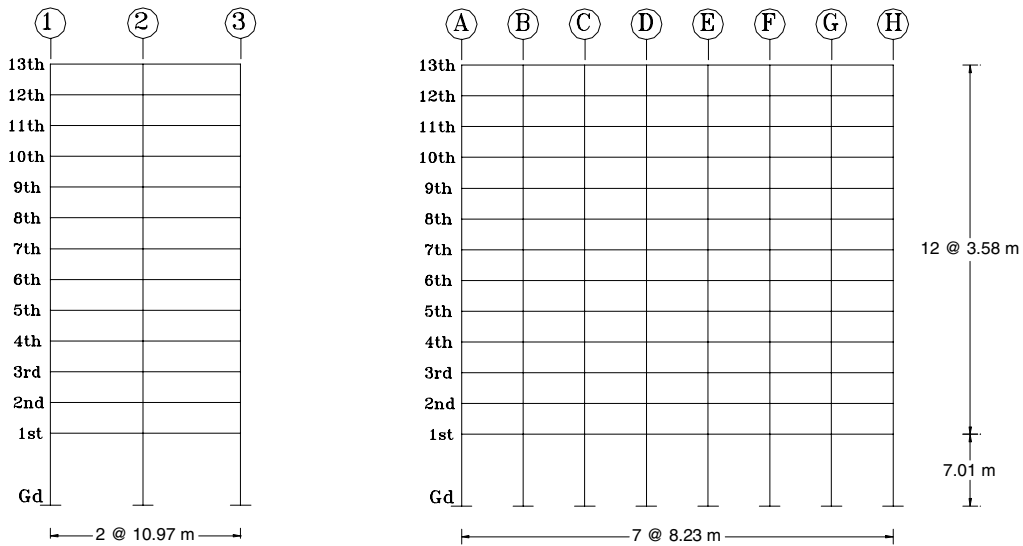


Figure 13. North-south and east-west elevation views of studied building

ANALYTICAL STUDY

The analytical study is conducted with an actual building to gain insight into (a) the size of the oval dampers needed to isolate the roof of a typical medium-rise building; (b) the magnitude of the lateral displacements experienced by the isolated roof; and (c) the effectiveness of the proposed isolation system in a

three-dimensional building with realistic dimensions and under realistic ground motions. As in the experimental study, the effectiveness of the proposed roof isolation system is assessed by computing the response of the analyzed building under the effect of two different ground motions and comparing these responses when the building is considered with and without the proposed isolation system.

Selected Building

The building selected for the analytical study is an existing commercial building located in Sherman Oaks, California and constructed around 1964. As shown in Figures 12 and 13, the building has 13 stories, a rectangular plan 22 meters (72 feet) wide and 58 meters (189 feet) long, and built with moment-resisting reinforced-concrete frames. It has seven bays of 8.23 m (27 feet) each along its longitudinal direction and two bays of 10.97 m (36 feet) each along its transverse direction. The floor system consists of a 102-mm (4-in), one-way reinforced concrete slab supported by reinforced concrete beams and girders. The dimensions and properties of its beams and columns are listed in Table 2. The nominal strengths of the concrete and reinforcing steel used in its design are 27.5 MPa (4,000 psi) and 412 MPa (60,000 psi), respectively. As one of the buildings instrumented by the California Division of Mines and Geology, acceleration records were obtained at its base and several other locations during the 1994 Northridge, California, earthquake (Shakal and Huang [15]). For the analysis, the building is considered with a gravity load (dead plus live) of 9.1 kN/m² (190 psf) for the floors and 8.4 kN/m² (175 psf) for the roof. In addition, all its structural elements are considered with their gross moments of inertia (neglecting flanges of T beams) and a modulus of elasticity of 24,000 MN/m² (3490 ksi). For the analysis, too, the beams and columns of the building are modeled with bilinear beams elements with yield moments calculated on the basis of the actual steel reinforcement in them. The damping matrix of the building is assumed, when considered without the roof isolation system, proportional to its stiffness and mass matrices, with a damping ratio of 2 per cent in its fundamental mode. The fundamental natural frequency of the building is 0.459 Hz along its longitudinal direction and 0.415 Hz along its transverse direction.

Table 2. Dimensions and properties of beams and columns of studied 13-story building

| Col- umn Line | Beams | | | | Columns | | | | |
|---------------------|-------|----------------|--------------------------|--------|---------------------|----------|-------|----------------|--------------------------|
| | Floor | Section (m) | Steel Rein- forcement | | Col- umn Line | Location | Story | Section (m) | Steel Rein- forcement |
| | | | Pos. | Neg. | | | | | |
| 1 & 3 | 1-4 | 0.46 x 0.99 | 4 # 8 | 6 # 8 | 1 & 3 | Interior | 1-4 | 0.61 x 0.91 | 10 # 9 |
| | 5-8 | 0.46 x 0.99 | 3 # 9 | 3 # 9 | | | 5-8 | 0.61 x 0.91 | 10 # 9 |
| | 9-13 | 0.46 x 0.99 | 3 # 9 | 3 # 9 | | | 9-13 | 0.61 x 0.91 | 10 # 9 |
| 2 | 1-4 | 0.61 x 0.81 | 4 # 8 | 5 # 11 | 1 & 3 | Exterior | 1-4 | 0.91 x 0.91 | 14 # 9 |
| | 5-8 | 0.61 x 0.81 | 3 # 8 | 5 # 10 | | | 5-8 | 0.91 x 0.91 | 14 # 9 |
| | 9-13 | 0.61 x 0.81 | 3 # 8 | 5 # 9 | | | 9-13 | 0.91 x 0.91 | 14 # 9 |
| A & H | 1-4 | 0.46 x 0.99 | 3 # 8 | 4 # 9 | 2 | Interior | 1-4 | 0.91 x 0.91 | 14 # 9 |
| | 5-8 | 0.46 x 0.99 | 3 # 8 | 5 # 8 | | | 5-8 | 0.91 x 0.91 | 14 # 9 |
| | 9-13 | 0.46 x 0.99 | 3 # 8 | 4 # 8 | | | 9-13 | 0.91 x 0.91 | 14 # 9 |
| B-G | 1-4 | 0.61 x 0.81 | 5 # 9 | 5 # 11 | 2 | Exterior | 1-4 | 0.61 x 0.91 | 10 # 9 |
| | 5-8 | 0.61 x 0.81 | 4 # 9 | 5 # 10 | | | 5-8 | 0.61 x 0.91 | 10 # 9 |
| | 9-13 | 0.61 x 0.81 | 3 # 8 | 6 # 9 | | | 9-13 | 0.61 x 0.91 | 10 # 9 |

Damper Design

As in the experimental study, the primary consideration in the selection of the properties and dimensions of the steel oval dampers for the roof isolation of the building is the need to form with the building's roof and the oval dampers an oscillator in resonance with the rest of building. More specifically, the damper's properties and dimensions are selected in a way that makes the dampers have an initial stiffness equal to

$$k_a = f^2 \omega_b^2 m_a \quad (2)$$

in which m_a is the roof mass, ω_b is the natural frequency of the building without its roof in radians per second, and f is the optimum tuning frequency ratio proposed by Sadek et al. [14], given by

$$f = \frac{1}{1 + \Phi_k m_a / M_b} \left[1 - \xi_b \sqrt{\frac{\Phi_k m_a / M_b}{1 + \Phi_k m_a / M_b}} \right] \quad (3)$$

where Φ_k denotes the amplitude at the level of the building's roof in the fundamental mode shape of the building without its roof (after the mode shape is multiplied by the corresponding participation factor), and M_b and ξ_b respectively are the generalized mass and damping ratio of the building in this same mode. Other important requirements considered in the design of the dampers include:

(1) The ability to have an ample fatigue life; that is, the dampers must tolerate a large number of large-deformation cycles without breaking or appreciably distorting.

(2) The ability to fit within the available space. That is, the dampers must fit in the space between columns after being fully deformed. Likewise, their vertical dimension should not be greater than the depth of the top-floor beams.

For the calculation of the dampers' initial stiffness using Equation 2, it is considered that the roof mass of the building is equal to 1,082 Mg (74.0 kip-s²/ft). This value includes the mass of the 102-mm (4-in) roof slab, roof beams, parapet, mechanical and electrical equipment, and all other appurtenances commonly found on a building's roof. Similarly, it is considered that in its fundamental mode and along its longitudinal direction, the building without its roof has a natural frequency of 0.481 Hz, a generalized mass of 12,756 Mg (872.6 kip-s²/ft), and a mode shape amplitude at roof level of 1.27; and that along its transverse direction these parameters are respectively equal to 0.435 Hz, 12,558 Mg (859.0 kip-s²/ft), and 1.29. Accordingly, it is found that the dampers need to provide a lateral stiffness of 7952 kN/m (488.7 kip/in) along the longitudinal direction and 6460 kN/m (397.0 kip/in) along the transverse direction.

Given the required initial stiffnesses, a basic damper is designed and the number of these basic dampers needed to provide such stiffnesses is determined as follows:

(1) A small value of the strain ϵ is chosen to enhance the chances of a good fatigue life; therefore, arbitrarily it is considered that $\epsilon = 1.25\%$. Given then that $\epsilon = e/2R$ and to obtain a reasonable value of the ovals' bent radius R , the thickness e of the low-carbon (SAE 1010) steel plate from which the ovals are to be made is selected as $e = 0.953$ cm (3/8 in). Therefore, the bent radius of the ovals is $R = e/2\epsilon = 0.953/(2 \times 0.0125) = 38.12$ cm (15 in). Additionally, a preliminary value of 20 cm (7.87 in) is assigned to the ovals' width b ; that is, $b = 20$ cm (7.87 in).

(2) The maximum force P that the basic damper is capable of developing is calculated according to Equation 1. Thus $P = \sigma b e^2 / 2R = (196200)(0.20)(0.00953)^2 / (2 \times 0.3812) = 4.674$ kN, where $\sigma = 19,6200$ kN/m² (28.43 ksi) is the true stress (corresponding to $\epsilon = 0.0125$) estimated from simple-tension tests of the steel grade from which the ovals are built. It should be noted that, according to experiments, for small strains ($0.002 < \epsilon < 0.01$), σ is close to the yield strength $\sigma_y = 179,500$ kN/m² (26 ksi); but for $\epsilon = 0.14$, σ is close to the ultimate strength $\sigma_u = 316,200$ kN/m² (45.8 ksi).

(3) The stiffness of the basic damper k_0 is calculated according to $k_0 = P/\delta_y$, where $\delta_y = R/100\gamma\epsilon$ is the peak elastic deformation of the damper. This is an empirical formula developed on the basis of numerous experiments performed on oval dampers over time. The γ factor is obtained from the following relation: $\gamma = 2.11-13.1\epsilon$, valid for low-carbon steel (SAE 1010), when $0.01 < \epsilon < 0.10$. Hence, $\delta_y = 0.3812 / (100 \times 1.95 \times 0.0125) = 0.1564$ m, and $k_0 = 4.674 / 0.1564 = 29.88$ kN/m.

(4) On the basis of the calculated stiffness for the basic damper, the number of dampers needed to supply the required stiffness in the longitudinal direction is $7952/29.88 = 266$, and that needed in the transverse direction is $6460/29.88 = 216$. It is concluded, however, that in both cases the required number of dampers is too high since it would be impossible to fit them in the available space between the building's columns.

(5) To diminish the required number of dampers, the width is increased to $b = 66.5$ cm (26.2 in) for the dampers in the longitudinal direction and $b = 67.5$ cm (26.6 in) for the dampers in the transverse direction, keeping all other dimensions the same. With this new width, the required number of dampers in the longitudinal direction is $(266)(20/66.5) = 80$, and that in the transverse direction is $(216)(20/67.5) = 64$. In both cases, it is now considered that the required number of dampers is acceptable.

(6) The aggregate force-deformation behavior of the 80 oval dampers acting in the longitudinal direction is approximated by a bilinear model similar to the one shown in Figure 6, where the coordinates of points K and M are (15.64 cm, 1243.7 kN)[6.157 in, 279.2 kip] and (120 cm, 1410 kN)[47.24 in, 316.5 kip], respectively. Note that 1243.7 kN = $(4.674$ kN)(66.5 cm/20 cm)(80) and that 1410 kN results from considering that the slope of line K-M in Figure 6 is 2% of the slope of line O-K. Similarly, the aggregate force-deformation behavior of the 64 oval dampers acting in the transverse direction is also approximated by the bilinear model shown in Figure 6, where the coordinates of points K and M are (15.64 cm, 1010.3 kN)[6.157 in, 226.8 kip] and (120 cm, 1145 kN)[47.24 in, 257.1 kip], respectively.

(7) From numerical simulations conducted with the force-deformation models defined in Step 6, it is found that the peak oval deformations under the ground motions described in the following section are in all cases less than ± 36.1 cm (± 14.2 in). Assuming, then, that this peak oval deformation is, to be on the safe side, ± 40 cm (15.7 in), and that A , the length of the straight portion of an oval from the attachment point to the start of the circular bend is equal to 1.35 times half the peak oval deformation (practical rule applied to keep ovals from distorting), one obtains $A = 1.35(40/2) = 27$ cm (10.6 in). The final dimensions of the basic oval damper are thus (see Figure 14): $R = 38.12$ cm (15.0 in), $e = 0.953$ cm (3/8 in), $b = 66.5$ cm (26.2 in) for dampers in the longitudinal direction and 67.5 cm (26.6 in) for dampers in the transverse direction, and $A = 27$ cm (10.6 in). The total length of the damper is 136.2 cm (53.6 in), allowing 5 cm (2.0 in) for attachment of the damper.

(8) It is functional to arrange the oval dampers in devices that contain four basic dampers each, such as shown schematically in Figure 15, then install each of these devices between two columns, connecting one of the hinges (A_1 or A_2) to a column and the other to the roof. A top view of the roof isolation system would show the devices as viewed in Figure 15, with 20 of them along the longitudinal direction and 16 of them along the transverse direction.

(9) Disregarding friction at connection points A_1 and A_2 , the peak axial force at these connection points during operation of the devices is approximately equal to $4.674 \times (67.5/20) \times 4 = 63.10$ kN (14.17 kip). This force of about 6.5 tons per device is relatively small and should facilitate the connection of the devices to the columns and to the roof without inducing unduly large stresses or deformations in the columns or the roof.

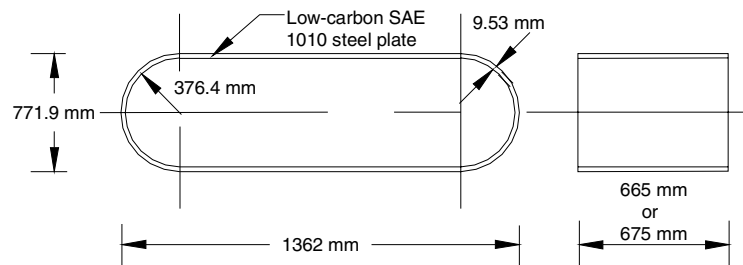


Figure 14. Dimensions of ovals considered in roof isolation of 13-story building

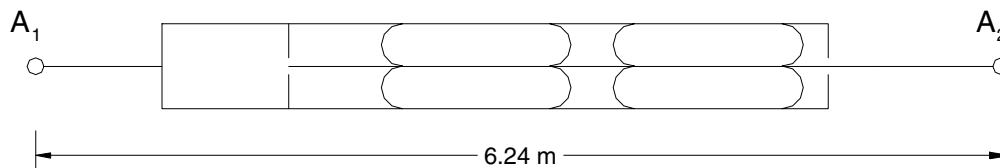


Figure 15. Schematic of four-oval-damper device (fully extended)

Selected Ground Motions

The ground motions considered in the analysis are (a) the ground motion recorded during the 1994 Northridge earthquake at ground level along the north-south (transverse) direction of the building being studied, and (b) the north-south component of the ground motion recorded at the Taichung-Wufeng station during the 1999 Taiwan earthquake. These ground motions, however, are modified to tune their dominant frequencies to the fundamental natural frequency of the building along the direction of analysis. In the case of the ground motion from the Northridge earthquake, the tuning is performed by multiplying the time axis of the original ground motion by a factor of 1.453 for the analysis of the building along its longitudinal direction and 1.600 for the analysis along its transverse direction. In the case of the ground motion from the Taiwan earthquake, these scale factors are respectively equal to 3.486 and 3.855. As in the experimental study, the ground motions are tuned to the fundamental natural frequency of the building because it is known (Villaverde and Koyama [13]) that the effectiveness of a vibration absorber is more evident under a resonant (damaging) ground motion than under a ground motion that only induces a low-level response.

The selected time histories are also modified to scale down their accelerations to a level that keeps the building in its linear range of behavior when it is implemented with the proposed roof isolation system. There are two reasons for scaling down the time histories this way. The first is to emphasize the grade and range of the roof isolation system's effectiveness, as vibration absorbers are more effective when a structure remains in its linear range of behavior at all times (Villaverde [1]). The second is to demonstrate that some earthquakes may damage a conventional building but not one implemented with the roof isolation system under investigation. The accelerations of the Northridge record are thus scaled down to a peak value of 0.192g when the analysis is performed along the longitudinal direction and 0.160 g when the analysis is performed along the transverse direction. Similarly, the accelerations of the Taiwan record are scaled down to peak values of 0.041g and 0.032g, respectively for the longitudinal and transverse directions.

Results

The results of the analysis are summarized in Tables 3 and 4. These tables show for each of the two excitations considered the story drifts obtained when the building is alternatively considered with and without the proposed roof isolation system. Shown in these tables too are the corresponding reductions attained with the use of the roof isolation system. On average, the roof isolation system reduces the story drifts of the building by 38.1 per cent in the longitudinal direction and 33.4 per cent in the transverse direction when the modified version of the acceleration record from the Northridge earthquake is considered. In the case of the modified version of the acceleration record from the Chi-Chi earthquake, these averages are 33.1 and 37.3, respectively. It may be seen, thus, that the roof isolation system significantly reduces the story drifts in the building. It is worthwhile to note, too, that although the building is kept in its linear range of behavior in all cases when it is considered with the roof isolation system, in all cases too some of the beams and columns of the building yield when the building is kept with its conventional configuration.

In regard to the response of the roof isolation system itself, it is found that under the modified version of the acceleration time history from the Northridge earthquake the oval dampers undergo a maximum deformation of 0.346 m (13.6 in) in the longitudinal direction and 0.323 m (12.7 in) in the transverse direction. In the case of the modified version of the acceleration time history from the Chi-Chi earthquake, the oval dampers are subjected to a maximum deformation of 0.361 m (14.2 in) along both the longitudinal and transverse directions. Thus, the maximum ductility demand on the oval dampers is equal to $0.361/0.1564 = 2.3$.

Table 3. Peak story drifts in 13-story building under modified 1994 Northridge acceleration record

| Story | Direction | | | | | |
|-------|-----------------------------|-------------------------------|---------------|-----------------------------|-------------------------------|---------------|
| | Longitudinal | | | Transverse | | |
| | Drift with no isolation (m) | Drift with roof isolation (m) | Reduction (%) | Drift with no isolation (m) | Drift with roof isolation (m) | Reduction (%) |
| 1 | 0.0564 | 0.0245 | 56.6 | 0.0495 | 0.0208 | 58.0 |
| 2 | 0.0257 | 0.0127 | 50.6 | 0.0223 | 0.0125 | 43.9 |
| 3 | 0.0205 | 0.0119 | 42.0 | 0.0186 | 0.0123 | 33.9 |
| 4 | 0.0164 | 0.0115 | 29.9 | 0.0163 | 0.0121 | 25.8 |
| 5 | 0.0157 | 0.0109 | 30.6 | 0.0150 | 0.0117 | 22.0 |
| 6 | 0.0161 | 0.0101 | 37.3 | 0.0141 | 0.0109 | 22.7 |
| 7 | 0.0150 | 0.0093 | 38.0 | 0.0139 | 0.0099 | 28.9 |
| 8 | 0.0131 | 0.0085 | 35.1 | 0.0137 | 0.0092 | 32.8 |
| 9 | 0.0124 | 0.0075 | 39.5 | 0.0128 | 0.0083 | 35.0 |
| 10 | 0.0110 | 0.0065 | 40.9 | 0.0115 | 0.0074 | 36.1 |
| 11 | 0.0086 | 0.0053 | 38.4 | 0.0097 | 0.0062 | 35.8 |
| 12 | 0.0063 | 0.0038 | 39.7 | 0.0074 | 0.0046 | 38.0 |
| 13 | 0.0042 | 0.0035 | 16.7 | 0.0051 | 0.0041 | 21.2 |

Table 4. Peak story drifts in 13-story building under modified 1999 Chi-Chi acceleration record

| Story | Direction | | | | | |
|-------|-----------------------------|-------------------------------|---------------|-----------------------------|-------------------------------|---------------|
| | Longitudinal | | | Transverse | | |
| | Drift with no isolation (m) | Drift with roof isolation (m) | Reduction (%) | Drift with no isolation (m) | Drift with roof isolation (m) | Reduction (%) |
| 1 | 0.0457 | 0.0241 | 47.3 | 0.0488 | 0.0200 | 59.0 |
| 2 | 0.0193 | 0.0119 | 38.3 | 0.0201 | 0.0115 | 42.8 |
| 3 | 0.0149 | 0.0106 | 28.9 | 0.0161 | 0.0107 | 33.5 |
| 4 | 0.0133 | 0.0099 | 25.9 | 0.0152 | 0.0101 | 33.6 |
| 5 | 0.0140 | 0.0091 | 35.1 | 0.0146 | 0.0094 | 35.5 |
| 6 | 0.0143 | 0.0084 | 41.1 | 0.0139 | 0.0086 | 37.8 |
| 7 | 0.0128 | 0.0078 | 39.4 | 0.0129 | 0.0078 | 39.7 |
| 8 | 0.0109 | 0.0070 | 35.7 | 0.0118 | 0.0070 | 40.8 |
| 9 | 0.0095 | 0.0062 | 34.8 | 0.0106 | 0.0063 | 40.9 |
| 10 | 0.0082 | 0.0053 | 35.1 | 0.0092 | 0.0054 | 40.7 |
| 11 | 0.0065 | 0.0044 | 32.4 | 0.0075 | 0.0046 | 38.2 |
| 12 | 0.0047 | 0.0036 | 23.3 | 0.0056 | 0.0039 | 30.0 |
| 13 | 0.0036 | 0.0031 | 13.2 | 0.0039 | 0.0034 | 12.5 |

CONCLUSIONS

The study reported herein shows that a roof isolation system implemented with steel oval elements may indeed be effective to reduce the seismic response of building structures. The experimental component of it further demonstrates that steel oval dampers may work well as energy dissipating devices and that they are capable of resisting large inelastic deformations without warping or a premature fatigue failure. Similarly, the analytical study reveals that the oval dampers required to implement the investigated roof isolation system in a typical medium-rise building are of reasonable dimensions relative to the size of the building and may be accommodated within the available space. Furthermore, it shows that the deformations to which these oval dampers may be subjected are within the range of the deformations they can resist without losing their load-carrying capacity. Thus, the proposed roof isolation system has the potential

to become a simple and inexpensive way to protect some buildings against earthquake effects and reduce, as a result, the amount of structural and nonstructural damage they may experience during a strong earthquake.

ACKNOWLEDGMENTS

This study was funded by a grant from the University of California Institute for Mexico and the United States (UC MEXUS) and Mexico's Consejo Nacional de Ciencia y Tecnología (CONACYT). The generous support from these two institutions is herein gratefully acknowledged. A word of appreciation is extended to UCI graduate student Samit Ray Chaudhuri, who effectively assisted in the conduction of the shake table tests and in the processing of the collected data. Thanks are also due to Alejandro Pérez Vargas of UNAM, who constructed the oval testing device and the tested steel oval dampers.

REFERENCES

1. Villaverde, R., "Roof isolation system to reduce the seismic response of buildings: A preliminary assessment," *Earthquake Spectra* 1998, **14**(3), 521-532.
2. Villaverde, R., "Aseismic roof isolation system: feasibility study with 13-story building," *Journal of Structural Engineering ASCE*, **128**(2), 188-196.
3. Villaverde, R. and Mosqueda, G., 1999 "Aseismic roof isolation system: analytic and shake table studies," *Earthquake Engineering and Structural Dynamics* 2002, **28**(3), 217-234.
4. Aguirre, M. and Chicurel, R., "Absorción de energía por flexión plástica," *Memoria del II Congreso de la ANIAC*, Academia Nacional de Ingeniería, Monterrey, N.L., Mexico, 1976, 617-631.
5. Aguirre, M. and Sánchez, A. R., "Disipadores de energía sísmica," *Construcción y Tecnología*, Instituto Mexicano del Cemento y del Concreto 1990, **III**(27), 15-19.
6. Aguirre, M. and Sánchez, A. R., "Structural seismic damper," *Journal of Structural Engineering, ASCE* 1992, **118**(5), 1158-1171.
7. Aguirre, M., "Device for control of building settlement and for seismic protection," *Journal of Geotechnical Engineering, ASCE* 1991, **117**(12), 1848-1859.
8. Aguirre, M. and Aguirre, R., "Anti-seismic structure: damper-equipped elastic frame," *Proc. Institution of Civil Engineers, Structures and Buildings* 2001, **146**(2), 147-151.
9. Skinner, R. I., Kelly, J. M., and Heine, A. J., "Energy absorption devices for earthquake resistant structures," *Proc. 5th World Conference on Earthquake Engineering*, Rome, Italy, 1973, **2** 2924-2933.
10. Skinner, R. I., Kelly, J. M., and Heine, A. J., "Hysteretic dampers for earthquake-resistant structures," *Earthquake Engineering and Structural Dynamics* 1975, **3**(3), 287-296.
11. Medeot, R., "Experimental testing and design of aseismic devices," *Proc. International Meeting on Earthquake Protection of Buildings*, Ancona, Italy, 1991, 59D-74D.
12. Parducci, A. and Medeot, R., "Special dissipating devices for reducing the seismic response of structures," *Proc. Pacific Conference on Earthquake Engineering*, Wairakei, New Zealand, 1987, 329-340.
13. Villaverde, R. and Koyama, L. A., "Damped resonant appendages to increase inherent damping in buildings," *Earthquake Engineering and Structural Dynamics* 1993, **22**(6), 491-507.
14. Sadek, F., Mohraz, B., Taylor, A.W. and Chung, R. M., "A method of estimating the parameters of tuned mass dampers for seismic applications," *Earthquake Engineering and Structural Dynamics* 1997, **26**(6), 617-635.
15. Shakal, A. F. and Huang, M. J., "Recorded ground and structure motions," Chapter 2 in Northridge Earthquake Reconnaissance Report, Vol. 1, *Earthquake Spectra* 1995, Supplement C to Volume 11.